Structure of a post-translationally processed heterodimeric double-headed Kunitz-type serine protease inhibitor from potato

Meulenbroek, E.M.; Thomassen, E.A.J.; Pouvreau, L.; Abrahams, J.P.; Gruppen, H.; Pannu, N.S.

research papers

Structure of a post-translationally processed heterodimeric double-headed Kunitz-type serine protease inhibitor from potato

**Elisabeth M. Meulenbroek,ª
Ellen A. J. Thomassen,ª
Laurice Pouvreau,b‡ Jan Pieter
Abrahams,ª Harry Gruppenb and
Navraj S. Pannuª***

ªBiophysical Structural Chemistry, Leiden
University, Einsteinweg 55, 2333 CC Leiden,
The Netherlands, and bLaboratory of Food
Chemistry, Wageningen University,
Bomenweg 2, 6703 HD Wageningen,
The Netherlands

‡ Present address: NIZO Food Research BV,
Kernhemseweg 2, 6718 ZB Ede,
The Netherlands.

Correspondence e-mail:
raj@chem.leidenuniv.nl

Potato serine protease inhibitor (PSPI) constitutes about 22% of the total amount of proteins in potato tubers (cv. Elkana), making it the most abundant protease inhibitor in the plant. PSPI is a heterodimeric double-headed Kunitz-type serine protease inhibitor that can tightly and simultaneously bind two serine proteases by mimicking the substrate of the enzyme with its reactive-site loops. Here, the crystal structure of PSPI is reported, representing the first heterodimeric double-headed Kunitz-type serine protease inhibitor structure to be determined. PSPI has a β-trefoil fold and, based on the structure, two reactive-site loops bearing residues Phe75 and Lys95 were identified.

1. Introduction

Protease inhibitors are abundantly present in plant seeds and tubers. In the tubers of the potato cultivar Elkana, for example, $\sim$50%(w/w) of the total soluble proteins are protease inhibitors (Pouvreau *et al.*, 2001). Plant protease inhibitors prevent pathogens or predators feeding on the plant by inhibiting their proteases. Protease inhibitors are therefore also expressed in response to wounding of the plant (for a review, see Valueva & Mosolov, 2004). In addition to their importance in plant physiology, protease inhibitors have also been reported to show anti-carcinogenic effects: they have been shown to prevent carcinogenesis in many different model systems and are effective at very low concentrations (for a review, see Kennedy, 1998).

Kunitz-type protease inhibitors can bind and inhibit serine, cysteine and aspartic proteases (Oliva *et al.*, 2010). Plant Kunitz-type protease inhibitors are small 20 kDa proteins that usually have two disulfide bonds and a single reactive site (single-headed), although two-reactive-site (double-headed) Kunitz-type inhibitors have also been described (*e.g.* Datta-gupta *et al.*, 1999; Azarkan *et al.*, 2011). The proteins inhibit proteases by binding tightly to the active site of the enzyme *via* their reactive-site loops in a substrate-like manner.

Potato serine protease inhibitor (PSPI) is the most abundant protease-inhibitor group in potato tubers and constitutes 42% of the protease inhibitors present in potato juice (Pouvreau *et al.*, 2003). This group of Kunitz-type serine protease inhibitors is composed of seven different isoforms that differ slightly in their pI values. PSPI has been reported to inhibit the serine proteases trypsin, chymotrypsin and human leukocyte elastase (Valueva *et al.*, 2000). It is expressed as a single polypeptide, but six amino acids are deleted during post-translational processing to yield a protein consisting of a large (16.2 kDa) and a small (4.2 kDa) subunit that are held

Table 1
Refinement and validation statistics for PSPI.

Values in parentheses are for the highest resolution shell.

| Data collection	
Space group	$P12_11$
Unit-cell parameters	a = 54.82, b = 93.92, c = 55.44, $\alpha = \gamma$ = 90.00, β = 100.69
Resolution (Å)	54.23–1.60 (1.69–1.60)
Resolution of a 100% complete data set† (Å)	1.80
Wilson plot B factor (Å²)	20.1
R_{merge}‡	0.044 (0.370)
$\langle I/\sigma(I)\rangle$	14.0 (1.8)
Completeness† (%)	70.0 (18.4)
Multiplicity	2.1 (1.8)
Total No. of observations	104501
No. of unique reflections	50787
No. of reflections in R_{free} set	2533
Refinement	
Resolution (Å)	54.23–1.60
No. of reflections	48229
No. of molecules in asymmetric unit	3
R_{work}/R_{free} (%)	16.8/22.1
No. of atoms	
Protein	4141
Ligand/ion	0
Water	504
B factors (Å²)	
Protein	24.2
Ligand/ion	N/A
Water	32.2
R.m.s. deviations	
Bond lengths (Å)	0.030
Bond angles (°)	2.25
No. of TLS bodies	3
Ramachandran favoured§ (%)	95.23
Ramachandran outliers§ (%)	0.38
Rotamer outliers§ (%)	0.88

† As calculated by *SFTOOLS* (B. Hazes, unpublished work). ‡ Multiplicity-weighted R_{merge} (Diederichs & Karplus, 1997; Weiss & Hilgenfeld, 1997). § As determined by *MolProbity* (Chen *et al.*, 2010).

together by a disulfide bridge and noncovalent interactions (Pouvreau *et al.*, 2003); the literature on Kunitz-type protease inhibitors refers to this multimeric complex as a 'dimer', but for clarity we refer to the complex as a heterodimer. PSPI is proposed to be a double-headed protease inhibitor, *i.e.* with two independent reactive-site loops, since it can form a ternary complex with both trypsin and chymotrypsin (Valueva *et al.*, 2000). These two loops, however, have never been identified. To determine the location of and the residues involved in the reactive-site loops and thus gain insight into the mechanism of PSPI, and since no three-dimensional atomic structure of a heterodimeric double-headed Kunitz-type protease inhibitor is known, we set out to determine the crystal structure of this protein. Here, we present the high-resolution structure of PSPI. The structure shows a β-trefoil fold with large protruding loops and, based on the structure, we identified the two reactive loops as being centred on Phe75 and Lys95.

2. Methods

Protein purification, crystallization and data collection have been reported previously (Thomassen *et al.*, 2004). The crystal diffracted to 1.60 Å resolution, but the data completeness at

this resolution was very low owing to the use of a square detector set to 1.8 Å, with only 18.4% completeness in the highest resolution shell (1.69–1.60 Å). Although incomplete, we included these high-resolution data in refinement because the $I/\sigma(I)$ levels were still good (>1.8) and we deemed it useful to include this high-resolution information. The resolution of the data corresponding to a 100% complete data set, as calculated by *SFTOOLS* (B. Hazes, unpublished work), was 1.80 Å. The phase problem was solved by molecular replacement with *BALBES* (Long *et al.*, 2008) using the structure of soybean trypsin inhibitor (Song & Suh, 1998) as a search model (the search model was chosen automatically by

(a)

(b)
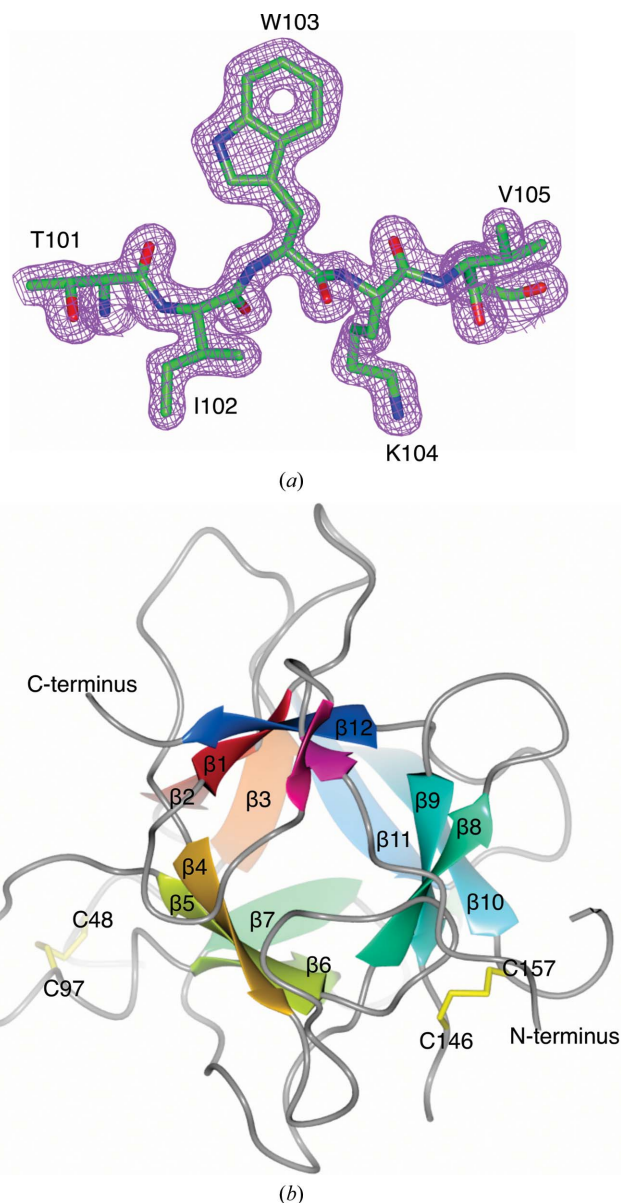
Figure 1
Overall structure of PSPI. (a) Representative part of the electron-density map of PSPI with a short stretch of the model (map clipped to show only this part of the model), demonstrating excellent electron density to high resolution. The map is contoured at 1.5σ. (b) Ribbon diagram of one molecule of PSPI with β-sheets indicated, showing a β-trefoil fold. The N- and C-termini are labelled as well as the two disulfide bridges (yellow).

BALBES; other search models such as the more similar PDB entry 3iir also give molecular-replacement solutions with, for example, the program *MOLREP*; Vagin & Teplyakov, 2010). The molecular-replacement solution was then rebuilt with *ARP/wARP* (Perrakis *et al.*, 1999), resulting in a model that was 87% complete. Refinement was performed with *REFMAC* using TLS (Murshudov *et al.*, 2011) and manual fitting was performed using *Coot* (Emsley *et al.*, 2010). Data and refinement statistics are shown in Table 1. In the analysis of the structure, superpositions with other Kunitz-type serine proteases and root-mean-square deviation calculations were performed using *THESEUS* (Theobald & Wuttke, 2006). Structure-based sequence alignment was performed with *VAST* (Thompson *et al.*, 2009). Atomic coordinates and structure factors have been deposited in the PDB (accession code 3tc2). Figures were prepared using *CCP4MG* (Potterton *et al.*, 2004).

3. Results and discussion

3.1. Overall structure

The structure of PSPI was determined to high resolution and contained three molecules in the asymmetric unit. These three molecules are very similar, with the root-mean-square deviations of the C^α backbone being 0.23 Å between subunits *A* and *B*, 0.33 Å between subunits *A* and *C* and 0.28 Å between subunits *B* and *C*.

The quality of the electron-density map is excellent for nearly all of the structure (Fig. 1*a*). The map is poor around the loops containing amino acids 42–46 in subunits *B* and *C* and amino acids 72–77 in subunits *A* and *B*. Nevertheless, for each of these loops an NCS-related subunit with moderate to good density (subunit *A* for loop 42–46 and subunit *C* for loop 72–77) was available to build a complete model. The well defined electron density found only in subunit *A* for loop 42–46 and in subunit *C* for 72–77 could not be attributed to any obvious interface interactions in the crystal.

The overall structure of PSPI shows a β-trefoil fold (Fig. 1*b*). It consists of 12 antiparallel β-strands which form six two-stranded β-hairpins. Three of these hairpins form a small β-barrel, while the other three hairpins close off the barrel in a triangular fashion. The β-strands are connected by long protruding loops. Two disulfide bridges are present: between Cys48 and Cys97 and between Cys146 and Cys157. This fold is usually observed for Kunitz-type serine protease inhibitors (*e.g.* soybean trypsin inhibitor; Song & Suh, 1998) and the reactive sites are commonly found in the protruding loops. The β-sheets provide a stable core that can hold together the structure, even if incision by the protease takes place, by both the covalent interaction of the disulfide bridges and the numerous noncovalent interactions.

Several structures of Kunitz-type serine protease inhibitors have previously been determined. The structures most similar to PSPI in terms of amino-acid sequence are a miraculin-like protein (PDB entry 3iir; Gahloth *et al.*, 2010), a Kunitz-type inhibitor from *Delonix regia* seeds (PDB entry 1r8n;

Table 2
Similarity of PSPI to other Kunitz-type protease inhibitors.

PDB entry	3iir	1r8n	2wbc	1avx
Sequence identity (%)	32.7	31.7	27.9	27.4
R.m.s. deviation of C^α backbone (Å)	1.47	1.22	1.21	1.35

Krauchenco *et al.*, 2003), a winged-bean chymotrypsin inhibitor (PDB entry 2wbc; Dattagupta *et al.*, 1999) and a soybean trypsin inhibitor (PDB entry 1avx; Song & Suh, 1998). Their sequence identities to PSPI are summarized in Table 2. A structure-based sequence alignment of PSPI with these proteins (Fig. 2) shows that the sequences are more similar in the β-strand regions, which form the scaffold of the structure, compared with the protruding loops which determine the specificity of the inhibitors. Structural superposition shows that the structures are indeed similar (see Table 2) but, as expected, the similarity is mostly in the β-sheet core, whilst the protruding loops differ substantially.

An important difference between PSPI and the previously determined structures of Kunitz-type serine protease inhibitors is that to the best of our knowledge PSPI is the first structure of a post-translationally modified heterodimeric double-headed protease inhibitor. Only crystal structures of monomeric Kunitz-type double-headed serine protease inhibitors are known, such as that of winged bean α-chymotrypsin inhibitor (Dattagupta *et al.*, 1999).

PSPI is expressed as a single polypeptide chain, but around six residues after Thr150 are removed in a post-translational process. Thus, there is no loop between Thr150 and Ser151 and, despite the consecutive numbering of the amino acids, there is also no peptide bond between Thr150 and Ser151 because of the deletion. The residues just before the site of the deletion (Thr149 and Thr150) and just after (Ser151, Ser152 and Asp153) are not modelled in our structure owing to poor density, probably caused by structural flexibility. Despite being (hetero)dimeric, the conformation of the whole molecule including the region close to the deleted loop is very similar to other, monomeric, Kunitz-type serine protease inhibitors. The structure seems to be held together in this very similar conformation by the disulfide bridge Cys146–Cys157 close to the beginning and the end of the deleted loop, since only the residues between these two cysteines show a different backbone direction from monomeric Kunitz-type serine protease inhibitors. Apparently, the presence of the extra loop and the post-translational deletion of this loop does not affect the overall structure of the inhibitor. It is possible that the loop functions as a shield for an important interface of the protein, leading to a (partially) inactive form which is activated upon cleavage. The range in which the excised loop can be present is indicated in Fig. 3(*a*).

3.2. Identification of reactive-site loops

The reactive-site loops of PSPI have not yet been identified. Previous predictions based on sequence alignment with other Kunitz-type inhibitors located the reactive-site loops around

Figure 2
Structure-based sequence alignment. Alignment of PSPI with other previously structurally characterized Kunitz-type serine protease inhibitors. β-Strands are indicated by blue arrows and the yellow box shows the six residues that were post-translationally deleted from PSPI.
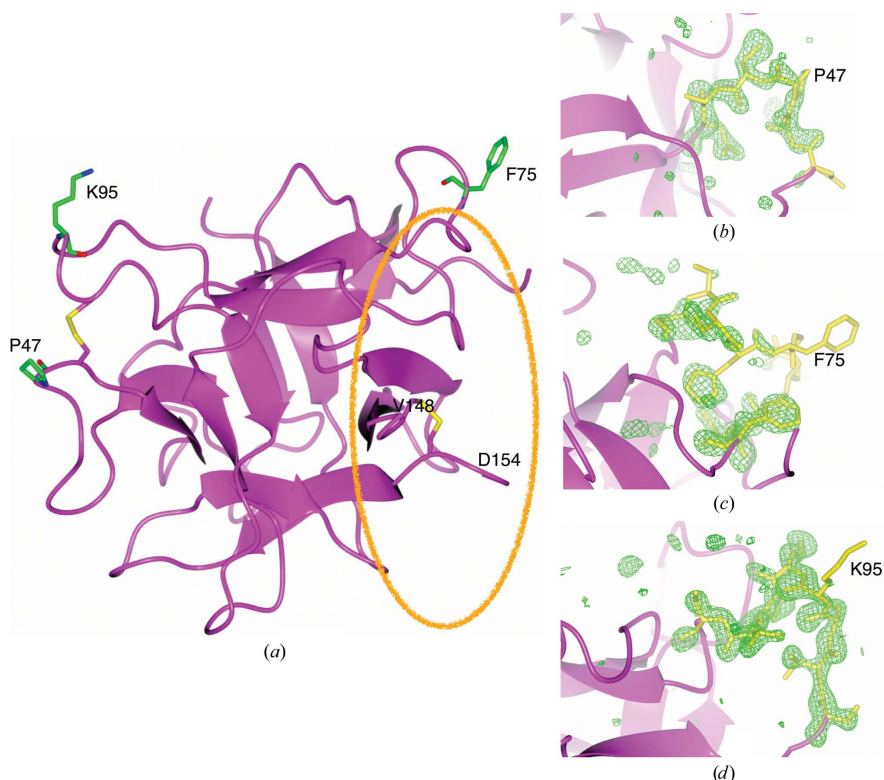
Figure 3
Reactive sites of PSPI. (*a*) P1 residues of the three most probable candidates for the reactive-site loops of PSPI highlighted on the structure of PSPI, showing their position to be in loops and showing how they stick out into the solvent. Disulfide bridges are indicated in yellow. The orange circle shows the range in which the excised loop may be present (on the right side of the protein in this view), and the last and first ordered residues in the structure at the beginning and the end of the excised loop are indicated (Val148 and Asp154, respectively). (*b*) OMIT map $(2F_o - F_c)$ of the putative reactive-site loop Asp45–Asn50 (yellow). (*c*) OMIT map $(2F_o - F_c)$ of the putative reactive-site loop Ser71–Phe80 (yellow). (*d*) OMIT map $(2F_o - F_c)$ of the putative reactive-site loop Ser92–Ser99 (yellow). The electron difference density maps are calculated based on phases from the model without the residues shown here in yellow and are contoured at 3σ.

Arg67-Phe68 (with Arg67 being in the P1 position) and around Met115-Leu116 (with Met115 occupying the P1 position; Valueva *et al.*, 2000). However, both of these proposed sites are located on the inside of the structure and not in protruding loops. Indeed, Arg67 is in the middle of a β-strand in the core of the protein and hence cannot be the P1 residue of the reactive-site loop. Similarly, there would also be a considerable amount of steric hindrance for a protease to bind if Met115 were a P1 amino acid.

To find more likely reactive-site loops, we compared the PSPI structure with those of other Kunitz-type serine protease inhibitors with previously determined and verified reactive-site loops. Five possibilities for reactive-site loops arose (I–V). Based on comparison with double-headed arrowhead protease inhibitor, the reactive loops could be located around Asn50 and around Leu84 of PSPI (possibilities I and II; Xie *et al.*, 1997). However, in the PSPI structure these residues are also not in protruding loops but at sterically more inaccessible positions, thus ruling out these sites.

Another possibility (III) for a reactive-site loop is near Asp45–Asn50 in PSPI (see Figs. 3*a* and 3*b*). This loop corresponds to the Asn38–Leu43 loop that has been proposed to be one of the reactive-site loops in winged bean α-chymotrypsin inhibitor (Datta-gupta *et al.*, 1999) based on structural similarity to its other verified reactive site. The Asp45–Asn50 loop in PSPI looks similar in structure and is partially similar in sequence to the winged bean α-chymotrypsin inhibitor reactive loop. The P1 residue in this loop is proline (Pro47 in PSPI) in both proteins. In PSPI this loop is partially disordered in subunits *B* and *C* and has higher than average *B* factors in subunit *A*. This is a typical property of

substrate loops that probably aids in binding the protease. The reactive-site loops adopt a more rigid conformation upon protease binding (Song & Suh, 1998).

The most common reactive-site loop for monomeric Kunitz-type serine protease inhibitors is the loop Ser71–Phe80, with Phe75 being the P1 residue in PSPI (possibility IV). This sequence has been proposed to be the reactive-site loop of other serine protease inhibitors, including miraculin-like protein (Gahloth *et al.*, 2010), a mutant trypsin inhibitor (based on a cocrystal with trypsin; PDB entry 3i29; S. Khamrui, S. Majumder, J. Dasgupta, J. K. Dattagupta & U. Sen, unpublished work), double-headed winged bean chymotrypsin inhibitor (based on biochemical evidence; Shibata *et al.*, 1998) and, finally, soybean trypsin inhibitor (based on a cocrystal with trypsin; Song & Suh, 1998). In PSPI this loop has poor density in subunits *A* and *B* and has high *B* factors in subunit *C*, indicating flexibility. As can be seen in Fig. 3(*a*), Phe75 sticks out into the solvent in subunit *C* (the only NCS-related molecule for which there is moderately good electron density; an OMIT map is shown in Fig. 3*c*), which would facilitate its recognition by a target protease.

The last possibility (V) for the reactive-site loop is around Lys95 in PSPI. The corresponding loop was identified to be a reactive-site loop in both double-headed arrowhead protease inhibitor (PDB entry 3e8l; R. Bao, C.-H. Jiang, C. W. Chi, S. X. Lin & Y. X. Chen, unpublished work) based on mutagenesis studies and a cocrystal with two trypsins (Bao *et al.*, 2009) and in barley α-amylase/subtilisin inhibitor based on a cocrystal with subtilisin savinase (Micheelsen *et al.*, 2008). The latter inhibitor was identified as the fifth most structurally related protein to PSPI by the *VAST* program. The loop around Lys95 has a similar conformation to the loop from the double-headed arrowhead protease inhibitor and protrudes from the structure, with Lys95 sticking out into the solvent as would be expected for a P1 reactive-site residue (Figs. 3*a* and 3*d*).
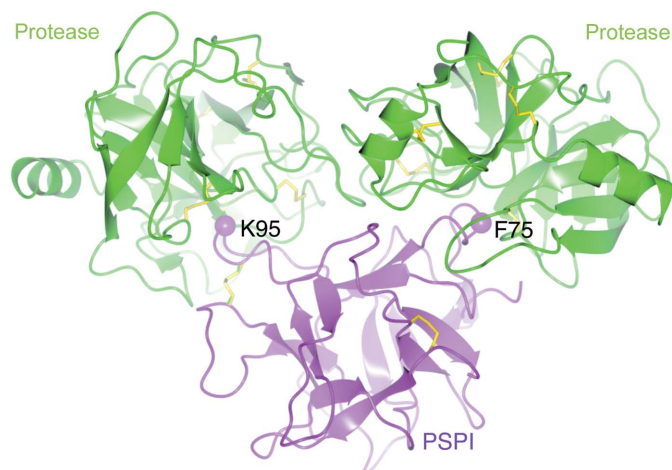
Figure 4
Model of PSPI (magenta) with two proteases (green) bound, showing that it is possible for two proteases to bind simultaneously to one molecule of PSPI at the reactive sites Phe75 and Lys95. In this picture two trypsins were modelled, but the picture will be equivalent for one chymotrypsin and one trypsin owing to the structural similarity of trypsin and chymotrypsin.

As stated above, the loops around Pro47, Phe75 and Lys95 are the three most likely candidates for reactive-site loops. Since a large positively charged amino acid fits best in the trypsin active site (to make contacts with Asp189), we propose that the Lys95 loop is the trypsin-interacting loop. Chymotrypsin is specific for sequences with bulky hydrophobic amino acids; hence, it is plausible that chymotrypsin binds to the Phe75 loop. Moreover, these two reactive-site loops have been confirmed by cocrystallization in other Kunitz-type serine protease inhibitors, providing stronger evidence for their potential biological function than the structural similarity of a loop in an uncomplexed structure, as is the case for the Pro47 loop. The Phe75 reactive-site loop might be hidden before post-translational processing of the loop between Thr150 and Ser151 (Fig. 3*a*).

It has been reported that one molecule of PSPI can bind a trypsin and a chymotrypsin molecule at the same time (Valueva *et al.*, 2000). To verify whether this is indeed possible with the suggested reactive-site loops, we modelled two proteases onto the reactive-site loops based on cocrystal structures in which a trypsin is bound to one of these loops (Song & Suh, 1998; Bao *et al.*, 2009) using the secondary-structure matching (SSM) function in *Coot*. As can be seen in Fig. 4, it is possible for the two proteases to simultaneously bind PSPI.

It has also been reported that PSPI inhibits human leukocyte elastase (Valueva *et al.*, 2000). Since elastase is specific for a small neutral amino acid, we are unsure whether it can act on either of the loops proposed for trypsin or chymotrypsin. Thus, it might require another binding site such as the Pro47 loop. Unfortunately, no elastase structure with a bound Kunitz-type serine protease inhibitor is available for comparison.

3.3. Interfaces for aggregation

The *PISA* (*Protein Interfaces, Surfaces and Assemblies*) server (Krissinel & Henrick, 2007) was used to investigate potential interfaces for interaction in the PSPI crystal structure. The surface including residues 107, 127 and 148 with the plane formed by residues 30, 58 and 169 was predicted to be a strong interface and to have a high probability of occurring in solution. Since PSPI has been reported to exist as a single molecule in solution (Pouvreau *et al.*, 2005), this interface is apparently not observed under ambient conditions. However, it has been reported that PSPI aggregates upon heating into a product with four molecules of PSPI (Pouvreau *et al.*, 2005). The interface that is detected by *PISA* could be the starting interface of such aggregation when the conditions for solubility are changed, as happens in a crystallization experiment with increasingly high concentrations, after which two seeding two-molecule PSPI complexes join to form an aggregate containing four molecules.

References

Azarkan, M., Martinez-Rodriguez, S., Buts, L., Baeyens-Volant, D. & Garcia-Pino, A. (2011). *J. Biol. Chem.* **286**, 43726–43734.

Bao, R., Zhou, C.-Z., Jiang, C., Lin, S.-X., Chi, C.-W. & Chen, Y. (2009). *J. Biol. Chem.* **284**, 26676–26684.

Chen, V. B., Arendall, W. B., Headd, J. J., Keedy, D. A., Immormino, R. M., Kapral, G. J., Murray, L. W., Richardson, J. S. & Richardson, D. C. (2010). *Acta Cryst.* D**66**, 12–21.

Dattagupta, J. K., Podder, A., Chakrabarti, C., Sen, U., Mukhopadhyay, D., Dutta, S. K. & Singh, M. (1999). *Proteins*, **35**, 321–331.

Diederichs, K. & Karplus, P. A. (1997). *Nature Struct. Biol.* **4**, 269–275.

Emsley, P., Lohkamp, B., Scott, W. G. & Cowtan, K. (2010). *Acta Cryst.* D**66**, 486–501.

Gahloth, D., Selvakumar, P., Shee, C., Kumar, P. & Sharma, A. K. (2010). *Arch. Biochem. Biophys.* **494**, 15–22.

Kennedy, A. R. (1998). *Pharmacol. Ther.* **78**, 167–209.

Krauchenco, S., Pando, S. C., Marangoni, S. & Polikarpov, I. (2003). *Biochem. Biophys. Res. Commun.* **312**, 1303–1308.

Krissinel, E. & Henrick, K. (2007). *J. Mol. Biol.* **372**, 774–797.

Long, F., Vagin, A. A., Young, P. & Murshudov, G. N. (2008). *Acta Cryst.* D**64**, 125–132.

Micheelsen, P. O., Vévodová, J., De Maria, L., Ostergaard, P. R., Friis, E. P., Wilson, K. & Skjøt, M. (2008). *J. Mol. Biol.* **380**, 681–690.

Murshudov, G. N., Skubák, P., Lebedev, A. A., Pannu, N. S., Steiner, R. A., Nicholls, R. A., Winn, M. D., Long, F. & Vagin, A. A. (2011). *Acta Cryst.* D**67**, 355–367.

Oliva, M. L., Silva, M. C., Sallai, R. C., Brito, M. V. & Sampaio, M. U. (2010). *Biochimie*, **92**, 1667–1673.

Perrakis, A., Morris, R. & Lamzin, V. S. (1999). *Nature Struct. Biol.* **6**, 458–463.

Potterton, L., McNicholas, S., Krissinel, E., Gruber, J., Cowtan, K., Emsley, P., Murshudov, G. N., Cohen, S., Perrakis, A. & Noble, M. (2004). *Acta Cryst.* D**60**, 2288–2294.

Pouvreau, L., Gruppen, H., Piersma, S. R., van den Broek, L. A. M., van Koningsveld, G. A. & Voragen, A. G. J. (2001). *J. Agric. Food Chem.* **49**, 2864–2874.

Pouvreau, L., Gruppen, H., van Koningsveld, G. A., van den Broek, L. A. M. & Voragen, A. G. J. (2003). *J. Agric. Food Chem.* **51**, 5001–5005.

Pouvreau, L., Gruppen, H., van Koningsveld, G., van den Broek, L. A. M. & Voragen, A. G. J. (2005). *J. Agric. Food Chem.* **53**, 3191–3196.

Shibata, H., Hara, S. & Ikenaka, T. (1998). *J. Biochem.* **104**, 537–543.

Song, H. K. & Suh, S. W. (1998). *J. Mol. Biol.* **275**, 347–363.

Theobald, D. L. & Wuttke, D. S. (2006). *Bioinformatics*, **22**, 2171–2172.

Thomassen, E. A. J., Pouvreau, L., Gruppen, H. & Abrahams, J. P. (2004). *Acta Cryst.* D**60**, 1464–1466.

Thompson, K. E., Wang, Y., Madej, T. & Bryant, S. H. (2009). *BMC Struct. Biol.* **19**, 33.

Vagin, A. & Teplyakov, A. (2010). *Acta Cryst.* D**66**, 22–25.

Valueva, T. A. & Mosolov, V. V. (2004). *Biochemistry*, **69**, 1305–1309.

Valueva, T. A., Revina, T. A., Mosolov, V. V. & Mentele, R. (2000). *Biol. Chem.* **381**, 1215–1221.

Weiss, M. S. & Hilgenfeld, R. (1997). *J. Appl. Cryst.* **30**, 203–205.

Xie, Z.-W., Luo, M.-J., Xu, W.-F. & Chi, C.-W. (1997). *Biochemistry*, **36**, 5846–5852.